Journal of Nuclear Materials 394 (2009) 155–159

Contents lists available at ScienceDirect

Journal of Nuclear Materials

journal homepage: www.elsevier.com/locate/jnucmat

Phase-field modeling of void lattice formation under irradiation

Shenyang Hu *, Charles H. Henager Jr.

Pacific Northwest National Laboratory, Richland, WA 99352, USA

ARTICLE INFO

Article history:
Received 4 May 2009
Accepted 4 September 2009

ABSTRACT

We, for the first time, propose a phase-field model to simulate the evolution of void ensembles under irradiation. The model takes into account one-dimensional migration of self-interstitial atoms (1-D SIA), vacancy diffusion, the generation and reaction between SIA and vacancies as well as the nucleation of voids. A one-dimensional random walker model (based on the theory of first-passage processes) is applied to describe the fast 1-D SIA while the Cahn–Hilliard equation is used to describe the slow three dimensional diffusion of vacancies. The coupling of these two methods greatly improves the computational efficiency for a system with strong inhomogeneity and anisotropy of diffusion. The formation of void lattices is simulated with the resultant model. It is found that a void lattice forms when the mobility of the 1-D SIA is four orders of magnitude larger than that of the vacancy mobility. A high generation rate of interstitials during displacement cascades delays the formation of a void lattice.

Published by Elsevier B.V.

1. Introduction

During the last three decades, numerous fully or partially ordered nanostructures and microstructures such as voids, gas bubbles, precipitates, and self-interstitial-atoms clusters have been observed in irradiated materials [1–11]. The implications of understanding the physical nature of this self-organization are quite clear from a technological perspective because material's thermo-mechanical properties strongly depend on the microstructure. It is expected that understanding and predicting the effect of irradiation conditions on microstructure and property evolution would lead to better approaches to the design of radiation-resistant materials and the optimization of nuclear plant operations.

Since the first observation of a void lattice in irradiated materials [1], many theoretical models have been proposed to explain the formation of ordered microstructures [12–17]. One important family of the models is based on an elastic energy minimization argument [17–20]. It is commonly accepted that the alignment of precipitates in elastically soft directions in alloys is driven by the minimization of elastic energy [21–24]. However, the void–void elastic interaction is strong only when they are within a few void diameters of each other. The elastic energy minimization argument cannot explain how voids organize themselves over relatively long distances, especially during the early stages of irradiation [12]. Another family of theoretical models is based on the fact that SIA and small SIA clusters preferentially migrate along close-packed directions or on close-packed atomic planes [25,26]. The particular migration direction causes void alignment because unaligned voids receive a larger flux of SIAs compared to aligned voids. As a result, the unaligned voids shrink while aligned voids nucleate and grow to form the void lattice. Woo and Frank [14,15] adapted this idea and described the evolution of void ensemble using the Fokker–Planck equation. The stability analysis of this nonequilibrium system shows that when the mean free path of a 1-D SIA becomes comparable with the average distance between the voids, two processes take place, i.e., the nucleation of voids is favored at the void lattice sites, and voids initially nucleated at position where neighboring voids are nonaligned will shrink. As a consequence, the void lattice forms. But this model is unable to predict the evolution of void ensembles. Heinisch and Singh [27] and Evans [13] simulated the formation of void lattices with 1-D SIA and 2-D SIA using Monte Carlo methods. However, the simulations were carried out under a number of assumptions for scaling the center of voids and the void size. In the present work, we propose a phase-field model for studying the evolution of a void ensemble in a solid with vacancy diffusion and 1-D migration of SIAs during irradiation. The advantage of the model is that the three dimensional evolution of a void morphology including the size distribution, shape and spatial distribution of voids can be obtained without artificially scaling the center and size of the voids.

2. Phase-field model of void evolution

Formation of the void lattice requires the migration and reaction of vacancies and interstitials produced by energetic particle radiation. Experiments [25,26] and molecular dynamics simulations [28–31] show that interstitials have much larger mobility than vacancies, and migrate along close-packed directions or on close-packed atomic planes. Therefore, the model should consider

* Corresponding author. Tel.: +1 509 376 4432; fax: +1 509 376 0418.
E-mail address: shenyang.hu@pnl.gov (S. Hu).

0022-3115/$ - see front matter Published by Elsevier B.V.
doi:10.1016/j.jnucmat.2009.09.002

both the slow and isotropic migration of vacancies and the fast and anisotropic migration of interstitials in order to correctly describe the evolution of a void ensemble. The Cahn–Hilliard equation is often applied to model systems that evolve via the diffusion of distinct species, where the inhomogeneity and anisotropy of a given species' diffusivity can be described by a diffusivity tensor. However, the time step is limited by the largest diffusivity or fastest moving species. The method is not efficient for a system with strong inhomogeneity and anisotropy of diffusion. Furthermore, it is hard to describe the directional migration with a diffusivity tensor.

In this work, we assume that (1) the diffusion of vacancies is driven by the gradients of chemical potential and vacancy concentration, and (2) the migration of SIAs follow the statistics of one-dimensional random walks. The model uses c_v (r,t) to describe the vacancy concentration and $c_{SIA}(r,t)$ to describe the concentration of SIAs. For the sake of simplicity in this first generation model, we only consider single vacancies and SIAs. It is straightforward to describe mobile vacancy clusters and interstitial clusters with related concentration variables. In the framework of the phase-field method, the diffusion of vacancies can be described by the Cahn–Hilliard equation [32],

$$\frac{\partial c_v(r,\ t)}{\partial t} = D_v \nabla \cdot \nabla \frac{\delta E(c_v(r,\ t))}{\delta c_v(r,\ t)} + \dot{g}_v(c_v(r,t)) - \dot{\gamma}(c_v(r,t), c_{SIA}(r,t)) \quad (1)$$

where $E = \int_V (F(c_v(r,t)) + \frac{\kappa}{2}(|\nabla c_v(r,t)|^2) dV$ is the total free energy of the system, including the chemical free energy $F(c_v(r,t))$ and the gradient energy. κ is the gradient coefficient associated with the void surface energy. The chemical free energy is a double-well potential which describes a two-phase system, i.e., a solid solution phase with an equilibrium vacancy concentration, c_v^{eq0}, and a void phase with an equilibrium vacancy concentration, c_v^{eq1}. D_v is the vacancy diffusivity. The second and third terms in Eq. (1) are the generation rate of vacancies and the reaction rate between vacancies and SIA, respectively. Eq. (1) is solved efficiently in Fourier space [33].

A one-dimensional random walker model is used to describe the directional migration of SIAs in this system [34]. In a continuum-space, continuum-time random walk starting at time $t = 0$ from the position $r_0 = 0$, the probability that the walker reaches the position r at time t is the solution (Green's function) of the diffusion equation

$$\frac{\partial p(r,t)}{\partial t} = D_{SIA} \Delta p(r,t) \quad (2)$$

with an initial condition $p(r,0) = \delta$ and boundary condition $p(r = \infty, t) = 0$. D_{SIA} is the diffusivity of an SIA. SIAs migrate along $< 1\,1\,0 >$ directions in FCC crystals. We assume the probability of migration along each $< 1\,1\,0 >$ direction is the same. For a given SIA distribution, $c_{SIA}(r,t)$ at time t, the change of SIA concentration, $\Delta c_{SIA}(r,t)$, after a time step Δt includes three contributions. The first contribution is the net flux along each of the 12 $< 1\,1\,0 >$ directions:

$$\Delta c_{SIA}(r,t) = \sum\nolimits_{k=1}^{12} \int_0^{R_k} \frac{1}{6} c_{SIA}(r_k,t)(p(dr_k,\Delta t) - p(0,0)\delta(r_k - r)) dr_k \quad (3)$$

The summation over k runs for 12 different $< 1\,1\,0 >$ directions, r'_k is a point on lines which pass through the point r and have one of the twelve $< 1\,1\,0 >$ directions, and $r'_k = |r'_k - r|$ is the distance between r and r'_k. $R_k = \min(\sqrt{D_{SIA}\Delta t}, R_K^0)$ is the minimum value of the mean free path $\sqrt{D_{SIA}\Delta t}$ of an SIA during the time step and R_k^0 the distance between the point r and the surface of the nearest void along the kth direction. The second contribution is the generation of SIAs $\dot{g}_{SIA}(c_v(r,t))\Delta t$, and the third contribution is the reaction between vacancies and SIAs $-\dot{\gamma}(c_v(r,t), c_{SIA}(r,t))\Delta t$, where the minus sign accounts for recombination reactions that reduce both vacancy and SIA concentrations. It is usually true that SIAs cannot penetrate through voids, such that SIAs accumulate on the boundaries of voids when SIAs approach voids. Therefore, if r is located on a void boundary,

$$\Delta c_{SIA}(r,t) = \sum_{k=1}^{12} \int_0^{R_k} \frac{1}{6} c_{SIA}(r'_k,t) \times \left(\int_{dr'_k}^{\sqrt{D_{SIA}\Delta t}} p(dr''_k,\Delta t) dr''_k - p(0,0)\delta(r'_k - r) \right) dr'_k \quad (4)$$

The summation runs over the 12 possible directions where the vacancy concentration at the first nearest point of the point r is lesser than 0.5. This means that r'_k is not a point belonging to a void. $\Delta c_{SIA}(r,t)$ will be zero if r is located inside of a void.

Coupling the Cahn–Hilliard Eq. (1) with the one-dimensional random walk model allows the evolution of vacancies and SIAs' to be simulated. The following thermodynamic properties are used in the simulations: the chemical free energy $F(c_v(r,t)) = -0.1(c_v(r,t) - 0.5)^2 + 0.205(c_v(r,t) - 0.5)^4$ which gives the equilibrium vacancy concentration $c_v^{eq0} = 0.006$ and $c_v^{eq1} = 0.994$ for the solid solution and void phases, respectively; the generation rates of vacancies and interstitials $\dot{g}_v(c_v(r,t)) = rand()\dot{g}_v^0$, and $\dot{g}_{SIA}(c_v(r,t)) = rand()\dot{g}_{SIA}^0$ if $c_v(r,t) \leqslant 0.1$, $\dot{g}_v(c_v(r,t)) = \dot{g}_v^0 e^{-(10c_v(r,t)-1)}$, and $\dot{g}_{SIA}(c_v(r,t)) = \dot{g}_{SIA}^0 e^{-(10c_v(r,t)-1)}$ if $c_v(r,t) > 0.1$ and a reaction rate $\dot{\gamma}(c_v(r,t), c_{SIA}(r,t)) = 0.5 c_v(r,t) c_{SIA}(r,t)$. $rand()$ is a random function which generates a number in the region $[0,1]$. Simulations are carried out in a $512\Delta x \times 512\Delta x$ two-dimensional simulation cell with about 400 randomly distributed small voids. The void diameter varies from $2\Delta x$ to $6\Delta x$, where Δx is the simulation grid spacing. The SIAs are assumed to migrate along $< 1\,1\,0 >$ and $< \bar{1}\,1\,0 >$ directions. The initial overall vacancy concentration is 0.05, and initial SIA concentration is zero. Void nuclei are randomly introduced at position r^* in the simulation cell if $c_v(r,t) < 0.5$ and $\int_\Omega c_v(r,t) dS > 8\Delta x^2$ in the region $\Omega : |r - r^*| \leqslant 15\Delta x$. The equilibrium vacancy concentration $c_v^{eq} = 0.994$ is assigned inside the void nucleus while its size is determined by total vacancy conservation in Ω and the equilibrium vacancy concentration of the solid solution phase $c_v^{eq0} = 0.006$. $t^* = D_v t/\Delta x^2$ is dimensionless time. A time step of $\Delta t^* = 0.1$ and gradient coefficient $\kappa^* = \kappa/\Delta x^2 = 0.1$ are used in the simulations.

3. Results

Fig. 1 shows the temporal evolution of a void ensemble for the case with the generation rates of vacancies and interstitials $\dot{g}_v^0 = \dot{g}_{SIA}^0 = 0.00001$ and $\frac{D_{SIA}}{D_v} = 10,000$ so that the diffusivity of 1-D SIAs is four orders of magnitude larger than that of vacancies. The color in the figure denotes the vacancy concentration. $c_v(r,t)$ is 1.0 in the red regions that represent voids and $c_v(r,t)$ is very small in the blue region (the matrix). The white A–A and B–B lines show $< 1\,1\,0 >$ and $< \bar{1}\,1\,0 >$ directions. The results demonstrate that a void lattice forms gradually. Tracking the evolution of individual voids, we find that (1) most surviving voids in the final void lattice are not exactly on final void lattice sites at the initial stage, rather they shift from their original positions to final lattice positions, (2) most voids away from lattice positions shrink because they are not in the shadow of neighbor voids, and face a larger interstitial flux, (3) shrinking voids cause an increase in local vacancy concentration and lead to new void nucleation near void lattice sites. The new nucleated void like the void labeled C in the Fig. 1 grows and becomes a void on a site in the perfect void lattice, and (4) larger voids on void lattice sites decrease their growth rate while smaller voids on lattice sites increase their

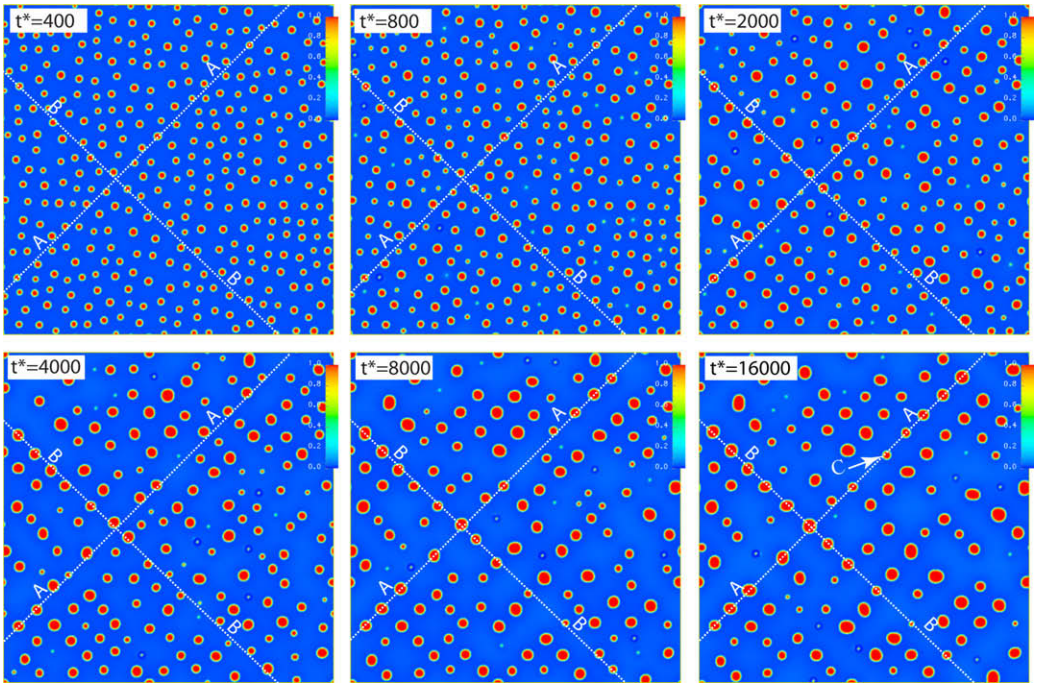

Fig. 1. Temporal evolution of a void ensemble for the case with generation rates of vacancies and interstitials $\hat{g}_v^0 = \hat{g}_{SIA}^0 = 0.00001$ and $\frac{D_{SIA}}{D_v} = 10,000$. The color in the figure denotes vacancy concentration. $c_v(r,t)$ is 1.0 in the red regions that represent voids. $c_v(r,t)$ is very small in the blue region (the matrix). The white A–A and B–B lines show $< 1\,1\,0 >$ and $< \bar{1}\,1\,0 >$ directions. (For interpretation of the references in color in this figure legend, the reader is referred to the web version of this article.)

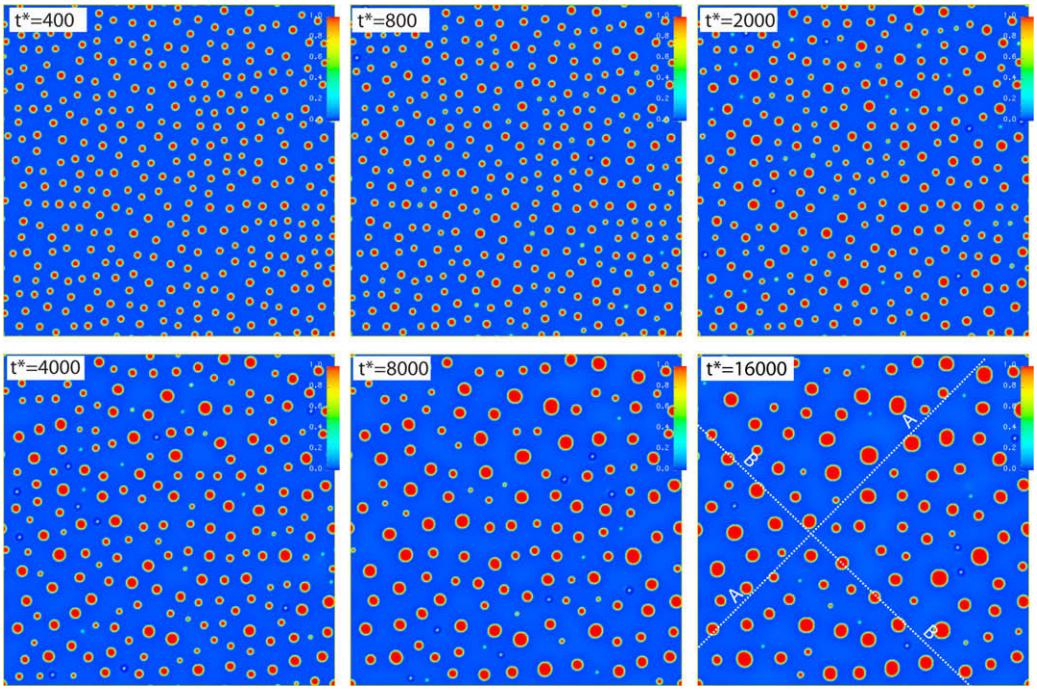

Fig. 2. Temporal evolution of a void ensemble for the case with generation rates of vacancies and SIAs $\hat{g}_v^0 = \hat{g}_{SIA}^0 = 0.00001$ and $\frac{D_{SIA}}{D_v} = 100$. The color in the figure denotes vacancy concentration as in Fig. 1 above. The white A–A and B–B lines show $< 1\,1\,0 >$ and $< \bar{1}\,1\,0 >$ directions. (For interpretation of the references in color in this figure legend, the reader is referred to the web version of this article.)

growth rate. These observations explain the formation of uniform void sizes in the void lattice. The simulation results confirm that the void lattice can be formed by slow and isotropic diffusion of vacancies, one-dimensional migration of SIAs, and continuous void nucleation. Theoretical models [14] predict that the void lattice will form when the mean free path of the one-dimensionally moving SIAs becomes comparable with the average distance between the voids at a sufficiently high void density. The mean free path can be calculated by $\lambda = \sqrt{D_{SIA}\tau_c}$, where τ_c is the mean lifetime or the average duration between consecutive changes of mobile and immobile interstitials or moving directions. Therefore, it is expected that the diffusivity of SIAs affect the formation of the void

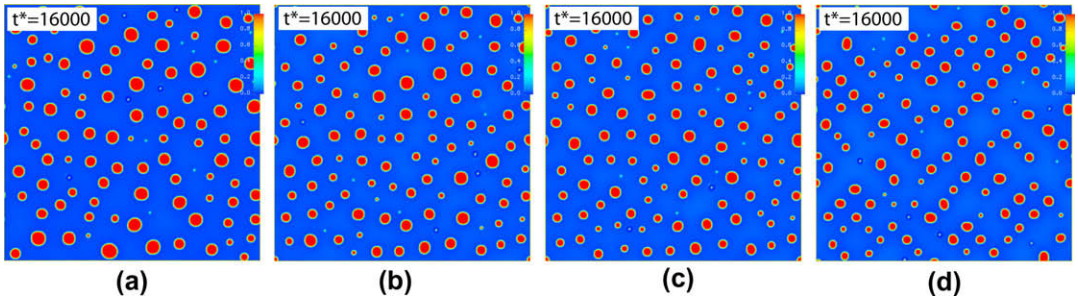

Fig. 3. Final void distributions for cases with generation rates of vacancies and SIAs $\dot{g}_v^0 = \dot{g}_{SIA}^0 = 0.00001$ and different diffusivity ratios $\frac{D_{SIA}}{D_v}$: (a) $\frac{D_{SIA}}{D_v} = 10$, (b) $\frac{D_{SIA}}{D_v} = 100$, (c) $\frac{D_{SIA}}{D_v} = 1000$, and (d) $\frac{D_{SIA}}{D_v} = 10,000$.

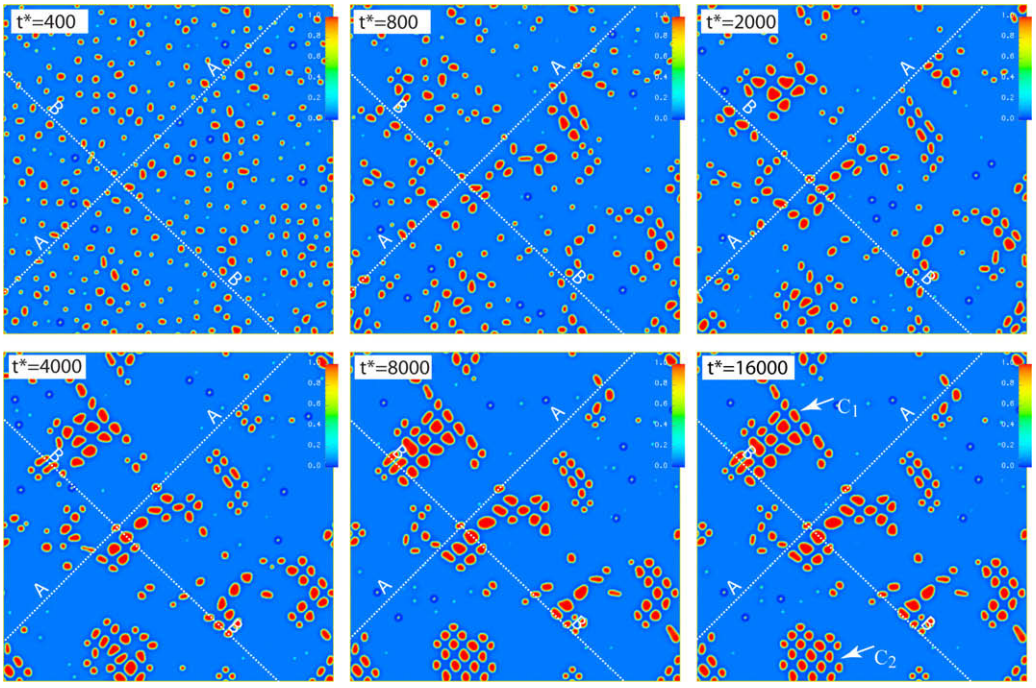

Fig. 4. Temporal evolution of a void ensemble for the case with generation rates of vacancies and SIAs $\dot{g}_v^0 = \dot{g}_{SIA}^0 = 0.002$ and $\frac{D_{SIA}}{D_v} = 10,000$. The color in the figure denotes vacancy concentration as before. The white A–A and B–B lines show $< 1\,1\,0 >$ and $< \bar{1}\,1\,0 >$ directions. (For interpretation of the references in color in this figure legend, the reader is referred to the web version of this article.)

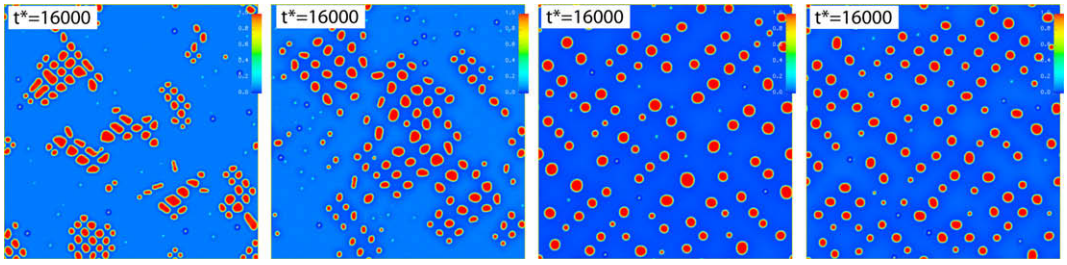

Fig. 5. Final void distributions for cases with diffusivity ratios $\frac{D_{SIA}}{D_v} = 10,000$ and different generation rates of vacancies and SIAs $\dot{g}_v^0 = \dot{g}_{SIA}^0$. (a) $\dot{g}_{SIA}^0 = 0.002$, (b) $\dot{g}_{SIA} = 0.0005$, (c) $\dot{g}_{SIA}^0 = 0.0001$, and (d) $\dot{g}_{SIA}^0 = 0.00001$.

lattice. With the same model parameters used in the simulation above except the diffusivity of SIAs, the simulation is repeated. Fig. 2 shows the temporal evolution of a void ensemble for the case with $\frac{D_{SIA}}{D_v} = 100$. We can find that no void lattice forms if the diffusivity of SIAs or the mean free lifetime is reduced. But short-range ordering of voids is observed in this case. Fig. 3 summarizes the final void microstructures as a function of SIA to vacancy diffusivity ratio. These results indicate that voids are distributed randomly when the SIAs' diffusivity is one order of magnitude larger than that of vacancies, i.e., $\frac{D_{SIA}}{D_v} = 10$. As the ratio $\frac{D_{SIA}}{D_v}$ increases the void

arrangement varies from short-range ordering to long-range ordering. A void lattice forms when $\frac{D_{SIA}}{D_v}$ reaches a critical value $\frac{D_{SIA}}{D_v} \approx 10^4$. The result confirms the theoretical prediction [14] that a critical mean free path ($\lambda = \sqrt{D_{SIA}\tau_c}$) exists for the formation of void lattices. Using the migration activation energy ΔQ_i of interstitials (0.08 eV) and vacancy (0.8 eV) in Fe [27], we can calculate the diffusivity $D_i = D_0 \exp(-\frac{\Delta Q_i}{k_B T})$. It is found that $\frac{D_{SIA}}{D_v}$ is about 10^4 at the temperature range between 700 and 900 K which is a typical operation temperature of nuclear plant component materials.

Next we study the effect of the generation rate of surviving interstitials and vacancies during the displacement cascade on void lattice formation. Fig. 4 shows the evolution of a void ensemble with a generation rate $\dot{g}_v^0 = \dot{g}_{SIA}^0 = 0.002$ and a diffusivity ratio $\frac{D_{SIA}}{D_v} = 10,000$. A high generation rate of interstitials implies a high interstitial flux in the simulation cell. We can clearly see that isolated voids are more readily annihilated in this case whether they are near lattice sites or not. Only ordered void clusters, which have the same orientation as that of the void lattice, survive in this simulation. It is found that void shapes become more faceted and irregular if we compare Fig. 1 and Fig. 4. The annihilation, nucleation, and uniform growth of voids can be observed during the evolution of the cluster C_1 and C_2 shown in Fig. 4. The effect of generation rates of vacancies and interstitials on the formation of void lattices is summarized in Fig. 5. We conclude that increasing the generation rate of interstitials delays the formation of the void lattice for a given diffusivity ratio $\frac{D_{SIA}}{D_v} = 10,000$.

4. Conclusions

In summary, an efficient phase-field model is developed for investigating the formation of void lattices in metals involving vacancy diffusion and 1-D SIA migration during irradiation. The simulations predict the morphological evolution of a void ensemble, and can be used to explore the effect of thermodynamic and kinetic properties of defects, such as diffusivity and defect generation rates on the evolution of void microstructures. The model will be extended to study the effect of distributed dislocations, 2-D SIA migration, and the elastic interaction between defects on void formation by integrating previous phase-field models developed by our research group [24,35].

Acknowledgments

This work was supported at Pacific Northwest National Laboratory by the US Department of Energy. PNNL is operated for the US Department of Energy by Battelle Memorial Institute under Contract DE-AC06-76RLO 1830.

References

[1] J.H. Evans, Nature 229 (1971) 403.
[2] K. Abe et al., Mater. Trans. Jim 34 (1993) 1137.
[3] T. Klemm, W. Frank, Appl. Phys. A: Mater. Sci. Process. 63 (1996) 19.
[4] P.B. Johnson, D.J. Mazey, J. Nucl. Mater. 218 (1995) 273.
[5] H.K. Sahu, K. Krishan, Pramana – J. Phys. 38 (1992) 685.
[6] D.J. Mazey, J.H. Evans, J. Nucl. Mater. 138 (1986) 16.
[7] J.O. Stiegler, K. Farrell, Scripta Metall. Mater. 8 (1974) 651.
[8] S.L. Sass, B.L. Eyre, Philos. Mag. 27 (1973) 1447.
[9] G.L. Kulcinsk, J.L. Brimhall, He. Kissinge, Trans. Am. Nucl. Soc. 13 (1970) 555.
[10] W. Jager, H. Trinkaus, J. Nucl. Mater. 205 (1993) 394.
[11] S.J. Zinkle, B.N. Singh, J. Nucl. Mater. 283 (2000) 306.
[12] N.M. Ghoniem, D. Walgraef, S.J. Zinkle, J. Comput.-Aided Mater. Des. 8 (2001) 1.
[13] J.H. Evans, Philos. Mag. Lett. 87 (2007) 575.
[14] C.H. Woo, J. Nucl. Mater. 276 (2000) 90.
[15] A.A. Semenov, C.H. Woo, W. Frank, Appl. Phys. A: Mater. Sci. Process. 93 (2008) 365.
[16] J.D. Torre et al., Philos. Mag. 85 (2005) 549.
[17] H.C. Yu, W. Lu, Acta Mater. 53 (2005) 1799.
[18] V.I. Dubinko, J. Nucl. Mater. 178 (1991) 108.
[19] V.I. Dubinko et al., J. Nucl. Mater. 161 (1989) 57.
[20] V.I. Dubinko, A.A. Turkin, Appl. Phys. A: Mater. Sci. Process. 58 (1994) 21.
[21] H. Nishimori, A. Onuki, Phys. Rev. B: Condens. Matter Mater. Phys. 42 (1990) 980.
[22] C. Sagui, A.M. Somoza, R.C. Desai, Phys. Rev. E: Stat. Nonlinear, Soft Matter Phys. 50 (1994) 4865.
[23] Y. Wang, L.Q. Chen, A.G. Khachaturyan, Acta Metall. Mater. 41 (1993) 279.
[24] S.Y. Hu, L.Q. Chen, Acta Mater. 49 (2001) 1879.
[25] M. Kiritani, J. Nucl. Mater. 206 (1993) 156.
[26] Y. Satoh, H. Matsui, T. Hamaoka, Phys. Rev. B: Condens. Matter Mater. Phys. 77 (2008) 094135.
[27] H.L. Heinisch, B.N. Singh, Philos. Mag. 83 (2003) 3661.
[28] B.D. Wirth et al., J. Nucl. Mater. 244 (1997) 185.
[29] N. Soneda, T.D. De la Rubia, Philos. Mag. A 81 (2001) 331.
[30] Y.N. Osetsky et al., J. Nucl. Mater. 276 (2000) 65.
[31] Y.N. Osetsky et al., J. Nucl. Mater. 307 (2002) 852.
[32] J.W. Cahn, Acta Metall. 9 (1961) 795.
[33] L.Q. Chen, J. Shen, Comput. Phys. Commun. 108 (1998) 147.
[34] T. Opplestrup et al., Phys. Rev. Lett. 97 (2006) 230602.
[35] S.Y. Hu, L.Q. Chen, Acta Mater. 49 (2001) 463.